CHAPTER 06 Experimental study of FZ-TIG welding

6.1 Preamble

The present chapter discuss the adoptability of Flux Zone TIG (FZ-TIG) welding to weld 2205 DSS. To apply FZ-TIG welding and analyze the effect of selected eight unique combinations of flux on weld bead geometry macrostructure study is performed. After identifying the perfect combination (outer and inner region) flux for FZ-TIG welding comparison of A-TIG, FB-TIG and FZ-TIG weld are observed concerning weld geometry. Moreover, the effect on mechanical properties (tensile strength and microhardness), electrode geometry and weld bead appearance has been reported in A-TIG, FB-TIG and FZ-TIG 2205DSS weld metal under the same welding conditions.

6.2 Purpose of adopting Flux Zone TIG (FZ-TIG) welding

FB-TIG welding is capable enough to increase the penetration by overcoming the disadvantages of A-TIG welding process by producing a clean surface appearance. However, the slight reduction in D/W ratio is reported in FB-TIG 2205 DSS weld metal compared to A-TIG weld metal at constant weld parameters as shown in Figure 0.1. This is due to flux gap (less amount of activated flux) reducing the oxygen level in the weld pool and thereby weak reversal Marangoni convection is formed compared to A-TIG welding process.
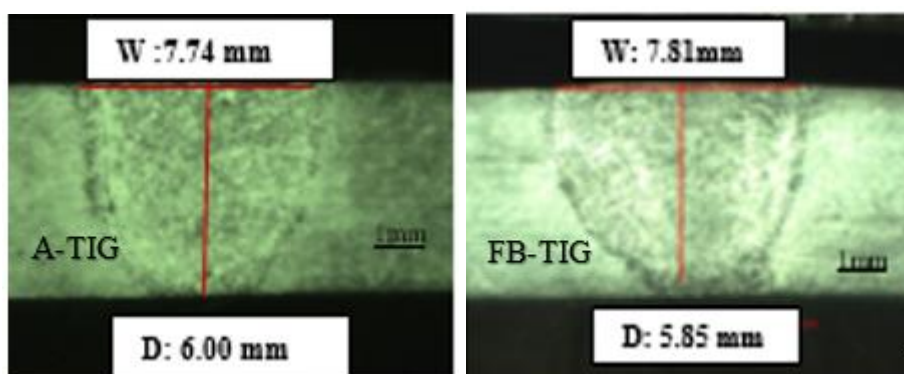

Figure 0.1 Macrostructure of A-TIG weld metal (D/W: 0.77) and FB-TIG weld metal (D/W: 0.74)

Flux Zoned TIG welding (FZ-TIG) is another novel variant of the A-TIG welding process based on the theory of arc constriction. In this process, two different activated

flux is applied in the centre and side regions of the weld surface before welding. Centre region flux easily evaporates during the welding and forms the constrict arc due to the negative ion of activated flux. Moreover, the activated flux applied in the centre region reverse the Marangoni convection and increases the penetration. Flux applied in the side region act as an insulator and forms the arc more constrict. Therefore, the combined effect of constriction of the arc due to negative ion and insulating effect along with reversal Marangoni convection increases the penetration. Huang et al. (2012) reported the comparison of alternative current TIG, A-TIG, FB-TIG and FZ-TIG weld joints in aluminium alloys. Among all these four processes highest D/W ratio was achieved in FZ-TIG weld joint along with satisfying mechanical properties. Rana et al. (2020) also performed a comparative study of aforementioned all welding processes on oxygen-free copper. The FZ-TIG welding is suggested as the best technique to bring out the utmost DOP. However, no study has been reported on FZ-TIG welding of stainless steel alloys. Therefore, FZ-TIG, the welding process is applied to weld 2205 DSS. To apply the FZ-TIG welding, eight combination of activated fluxes for the centre and side region are selected as mentioned in chapter 3.

6.3 FZ-TIG welding trial experiments

The specimens of 2205 DSS for the butt weld trials are cut and machine to $100 \times 100 \times 6$ mm 2205 DSS. To perform the FZ-TIG welding eight unique combinations of fluxes are mentioned in Table 4.2. Before welding, the specimen surface is cleaned with acetone to remove the oil contamination. The flux is mixed with acetone and stirred until it is dissolved to form a paste. This paste is evenly applied using a paint brush onto the weld bead surface till the whole measured quantity of flux spread uniformly by maintaining the coating thickness of 0.15 mm on the base metal. The 4 mm gap is maintained for the two side region and centre region. The selected flux combination is applied in two side regions and centre regions as shown in Figure 0.2.
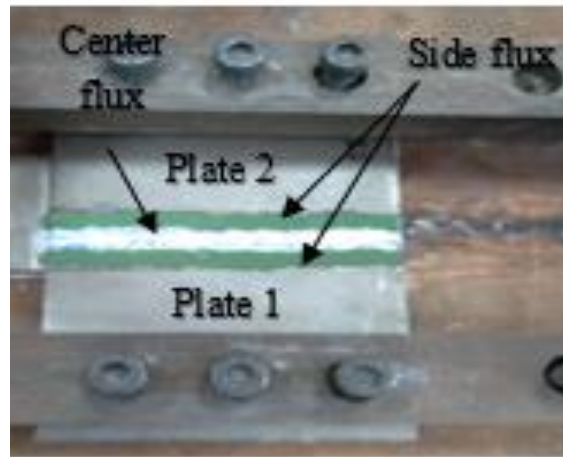
Figure 0.2 Flux applied in FZ –TIG welding

To perform the FZ –TIG welding, a constant welding current of 185 amps, a welding speed of 120 mm/min are selected. The other constant parameters such as shielding gas, flow rate, arc length, etc. are already mentioned in Table 4.2. After performing FZ-TIG welding, extracted traverse section of weld metal macrostructure examination is performed.

6.3.1 Effect of flux on weld bead geometry

Enhancement of weld penetration by activated flux is quite a complex phenomenon. As every flux has unique chemical and physical properties which affect the mechanisms differently and consequently affect weld bead geometry. The amount of heat flux density generated during welding also depicts the weld D/W ratio which governs the quality of the weld (Rana, et al., 2021). Heat input for all experiments is calculated by the equation (5.1) as mentioned in chapter 5. The variations in arc voltage and heat input are due to distinct properties of fluxes mentioned in Table 3.3. Moreover, the effect on penetration depth and D/W ratio are also summarized in Table 0.1.

Table 0.1 Effect of selected fluxes on heat input and weld bead geometry

The selected centre and side region flux			Voltage (V)	Heat input (KJ/mm)	DOP (mm)	Width (mm)	D/W ratio
Notation	Centre	Side					
(a)	SiO_2	CaO	14.2	1.31	5.27	9.69	0.54
(b)	SiO_2	Al_2O_3	15	1.39	5.99	9.59	0.62

(c)	MoO_3	Cr_2O_3	14	1.30	4.27	10.5	0.40
(d)	MoO_3	TiO_2	14	1.30	4.01	10.21	0.39
(e)	SiO_2	TiO_2	16	1.48	6.10	9.00	0.67
(f)	SiO_2	Cr_2O_3	16.5	1.53	6.9	7.60	0.90
(g)	SiO_2	$TiO_2+Cr_2O_3$	16.2	1.50	6.21	7.70	0.80
(h)	SiO_2+MoO_3	$TiO2+Cr_2O_3$	15.5	1.31	5.5	8.67	0.63

The macrostructure of all FZ-TIG weld metal is demonstrated in Figure 0.3. In each eighth combination of flux, the weld bead shows the unequal D/W ratio due to the unique properties of fluxes. The least penetration (4.01mm) as well D/W ratio was noticed with MoO_3 centre region flux and TiO_2 outer region flux combination as demonstrated in Figure 0.3 (d). This may be due to the absence of depth-enhancing mechanisms. However, the fluxes with other mentioned (Table 0.1) combinations predominately observed higher penetration and D/W ratio. In a few selected combinations such as SiO_2 with TiO_2, SiO_2 with Cr_2O_3 and SiO_2 with $TiO_2+Cr_2O_3$ complete and secure penetration is noticed.
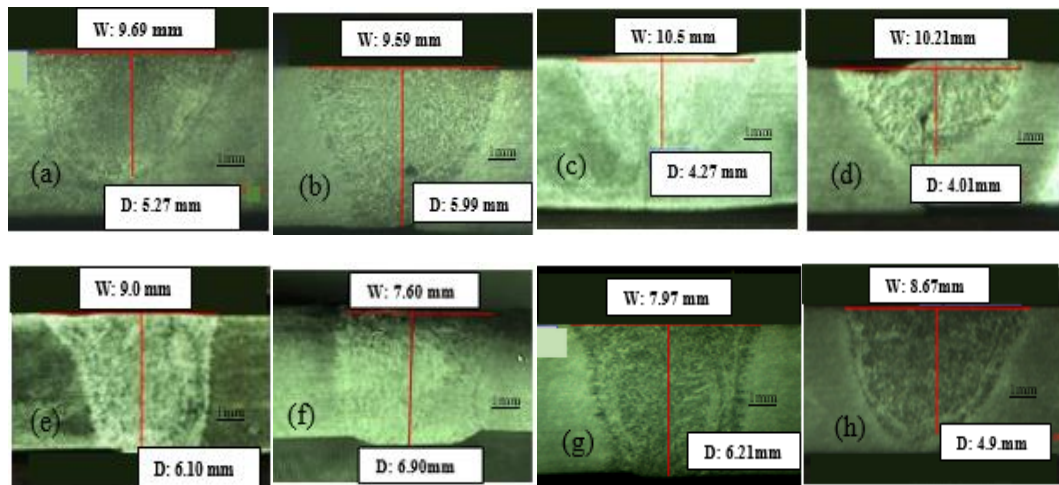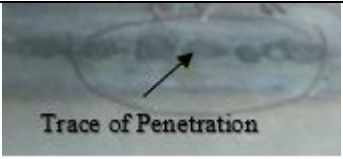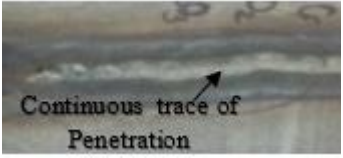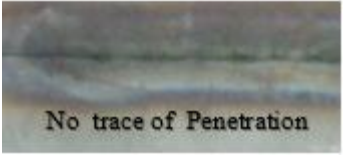

Figure 0.3 Macrostructure of FZ-TIG 2205 DSS weldments

Therefore, for the detail analyzes weld bead front and back surface study is also performed for these three cases as shown in Table 0.2. It is noticed that centre region flux SiO_2 and outer region flux $TiO_2 + Cr_2O_3$ do not indicate any trace of weld penetration on the back surface of the welded plate. Additionally, centre region flux SiO_2 outer region flux TiO_2 also does not indicate the continuous weld trace of penetration. This may be because of penetration enhancing mechanism was not adequate throughout the weld line. Lastly, centre region flux SiO_2 outer region flux

Cr_2O_3 back surface shows full and secure penetration evident throughout the weld line. Therefore, this combination of fluxes is deemed successful for FZ-TIG weld joint in 2205 DSS due to the sufficient depth enhancing mechanism established during the welding process.

Table 0.2 Weld surface appearance of FZ-TIG welded trial

Flux combination		Welded surface	
centre region flux	Side region flux	Front side	Back side
SiO_2	TiO_2		Trace of Penetration
SiO_2	Cr_2O_3		Continuous trace of Penetration
SiO_2	TiO_2 (50%) and Cr_2O_3 (50%)		No trace of Penetration

To compare the weld bead geometry and mechanical properties of FZ-TIG weld joint with A-TIG and FB-TIG weld joint, SiO_2 flux is selected as centre region flux and Cr_2O_3 flux is selected as side region flux. The experiments are performed at the aforementioned weld parameters. The SiO_2 flux is used to perform A-TIG welding process and the same flux with 2 mm flux gap is used to perform FB-TIG welding since maximum penetration is achieved with this flux and flux gap as noticed in chapter 4 (A-TIG) and chapter 5 (FB-TIG) respectively. Before A-TIG, FB-TIG and FZ-TIG welding selected fluxes are mixed with acetone in the required quantity and applied through a paint brush as shown in Figure 0.4.
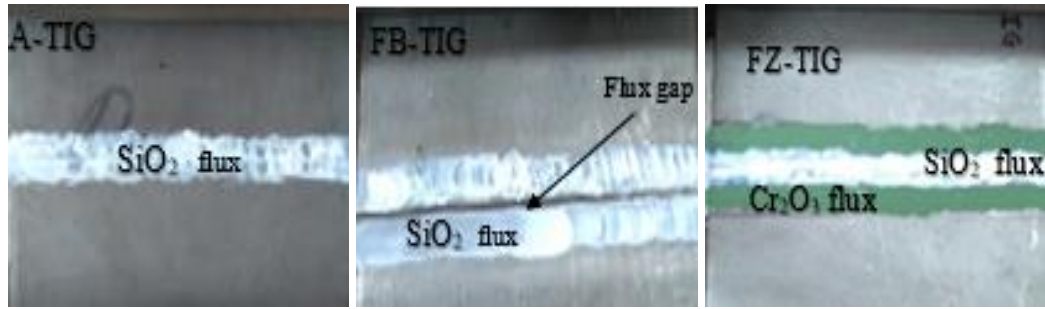
Figure 0.4 A-TIG, FB-TIG and FZ-TIG flux applied surface

6.4 Comparison of A-TIG, FB-TIG and FZ -TIG weld joint

6.4.1 Weld bead geometry

To compare A-TIG, FB-TIG and FZ-TIG weld bead geometry the traverse cross-section of the weld joint is cut, polished and etched as per the standards procedure explain in chapter 3. The macrostructures of A-TIG, FB-TIG, FZ-TIG (on a 6 mm thick plate) are demonstrated in Figure 0.5. Comparable penetration is reported in A-TIG and FB-TIG weld however, higher bead width is observed in FB-TIG weld than A-TIG weld. This is because in FB-TIG weld lesser amount of flux decomposes and thereby lesser will be the oxygen contained in the weld pool and reversal Marangoni convection become weak compared to A-TIG welding process. The highest penetration (6.9mm) along with a peak value of D/W ratio (0.90) is reported in FZ-TIG weld as shown in Figure 0.6. This is attributed to strong arc constriction due to negative electron and insulation effect and reversal Marangoni convection. This is 18 % more than A-TIG and 23 % FB-TIG weld metal.
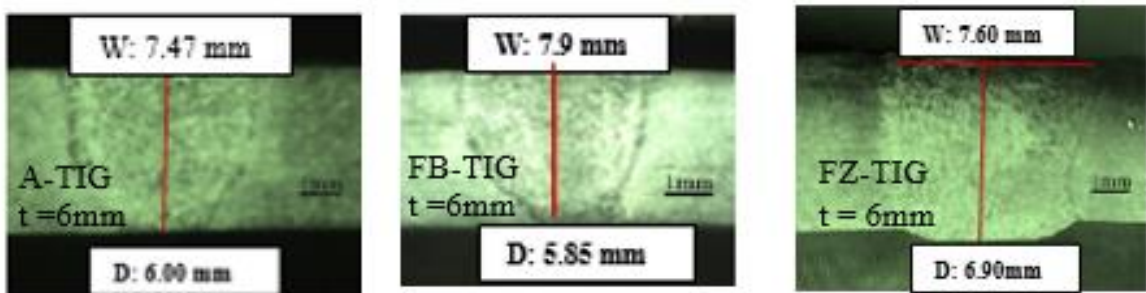

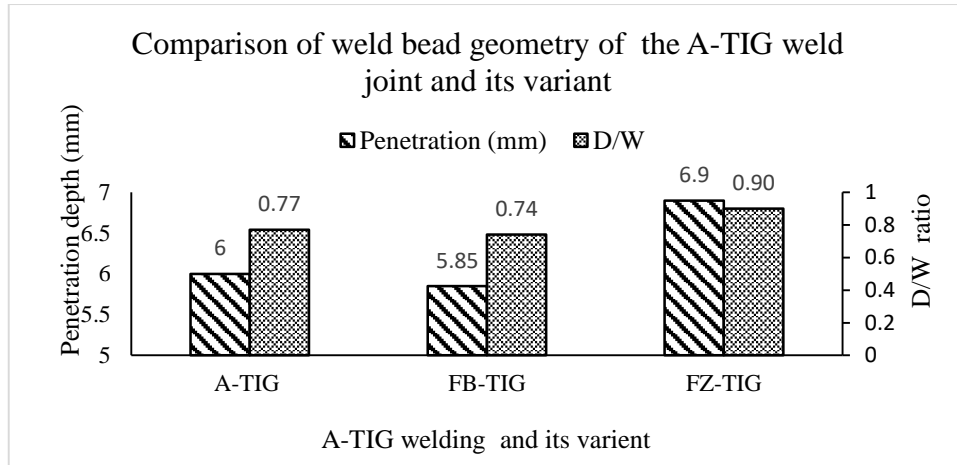Figure 0.5 Comparison of the macrostructure of TIG and its variants

Figure 0.6 Comparison of weld bead geometry of the TIG welding variant

Hence, further FZ-TIG welding is performed on 8 mm thick 2205 DSS to analyze the performance at the aforementioned weld parameters used for a 6 mm thick plate. The macrostructure of 8 mm thick plate is demonstrated in Figure 0.7.
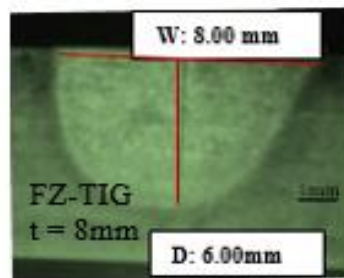

Figure 0.7 The macrostructure of FZ-TIG weld joint in 8 mm thick 2205DSS plate

D/W ratio achieved in 8 mm thick plate is less than the 6 mm thick butt weld. This is due to the heat dissipation area increasing with the plate thickness so, plate thickness affects adversely to D/W ratio. Similar, results are reported by Vidyarthy et al. (2016) in TIG weld joint by varying the plate thickness.

To understand the microstructure of A-TIG, FB-TIG and FZ-TIG weld metal optical microscopy is performed as per the standard procedure mentioned in the chapter3. During the A-TIG, FB-TIG and FZ-TIG welding applied activated flux increases the heat input and thereby the temperature of weld metal. Heat input is calculated in all welding conditions using equation 5.1 and mentioned in (Table 0.3). The highest heat input is observed in FZ-TIG welding 1.53 KJ/min this is attributed to the generation of high voltage due to strong arc constriction and reversal Marangoni convection.

Table 0.3 Welding process heat input

Welding Process	Flux	Voltage (amps)	Heat input (KJ/mm)
A-TIG	SiO_2	14.8	1.37
FB-TIG	SiO_2	14	1.30
FZ-TIG	SiO_2 and Cr_2O_3	16.5	1.53

Increase in heat input, reduce the cooling rate and the formation of delta ferrite to the austenite phase is complete. This results in lower ferrite in 2205 DSS and more balance austenite to ferrite ratio can be maintained which is the characteristic of DSS. The Figure 0.8 (a) – (d) shows the base metal, A-TIG, FB-TIG and FZ-TIG weld metal 2205 DSS microstructure respectively. The 2205 DSS base metal consists of an alternate layer of austenite (light gray) and ferrite (dark gray) represent in Figure 0.8(a). A-TIG, FB-TIG and FZ-TIG weld metal cool at room temperatures different austenite morphologies such as wedge-shaped Widmanstätten austenite, grain boundary austenite and intergranular precipitates in a matrix of ferrite as shown in Figure 0.8(b) - (d). In FB-TIG weld metal, thin laths of Widmanstätten austenite formation observed at grain boundaries in ferrite matrix compare to A-TIG and FB-TIG weld metal. This is due to due to lower heat input (lower diffusion rate) compare to A-TIG and FB-TIG weld metal (Table 3). Wherein, A-TIG and FZ-TIG weld metal due to higher heat input form the more balance structure of ferrite/austenite by forming larger laths of Widmanstätten austenite in a ferrite matrix. This may increase the mechanical strength of the 2205 DSS weld.
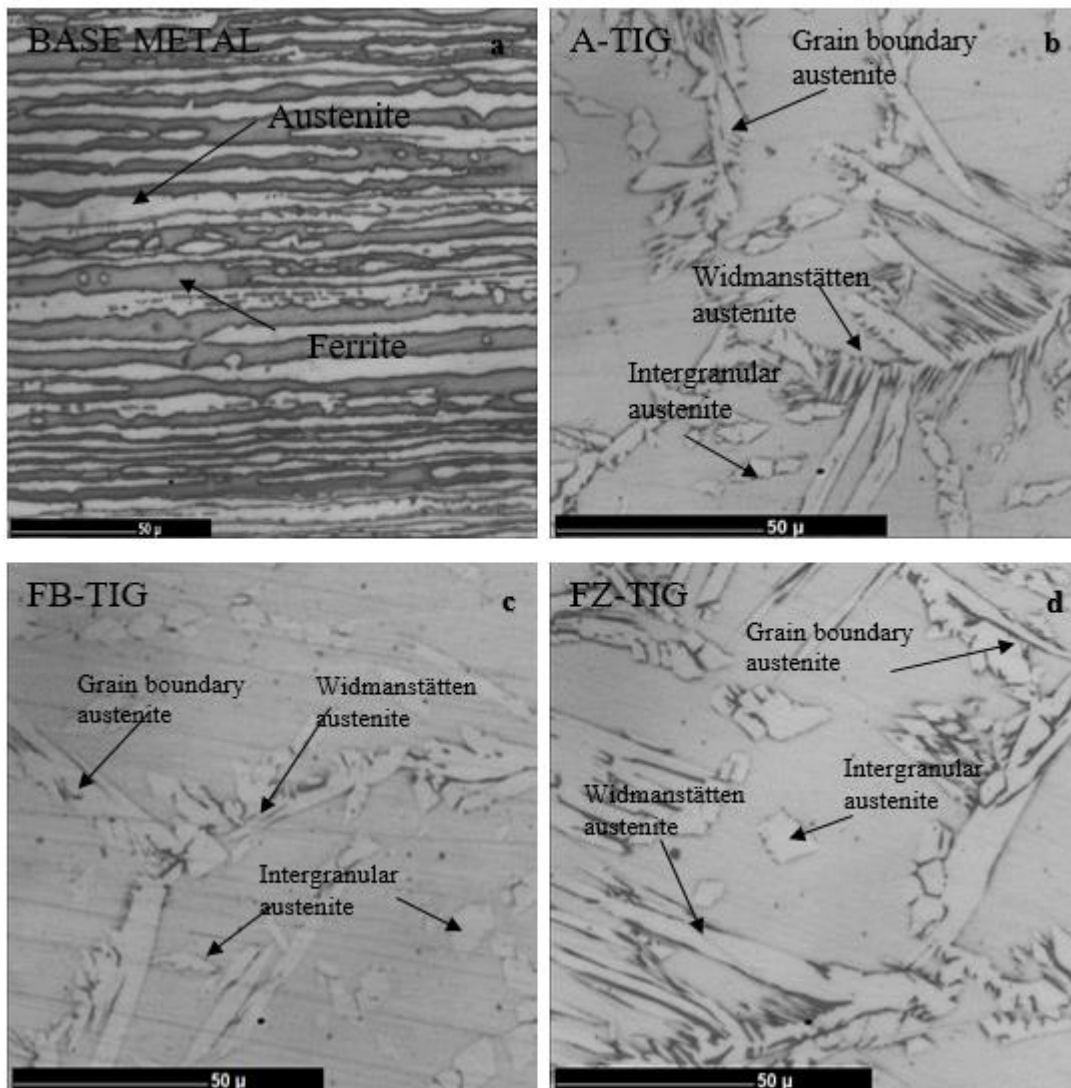
Figure 0.8 Optical microscopic image of (a) base metal (b)A-TIG (c) FB-TIG and (d) FZ-TIG welded samples

6.4.2 Mechanical properties

During the A-TIG, FB-TIG and FZ-TIG welding non-uniform expansion is take place which distorts the weld structure. The deviation in angular distortion is affected by penetration, bead width and plate thickness (Shyu, Huang, Tseng, & Chou, 2008) . The effect of distortion after A-TIG welding was reported by Vasantharaja et al. (2012) in 316LN stainless steel by vertical electronic height gauge. The angular distortion of A-TIG, FB-TIG and FZ-TIG welded plates is measured by a digital Vernier height gauge as shown in Figure 0.9. Figure 0.10 shows the effect of the D/W ratio on weld angular distortion in A-TIG, FB-TIG and FZ-TIG welding processes.
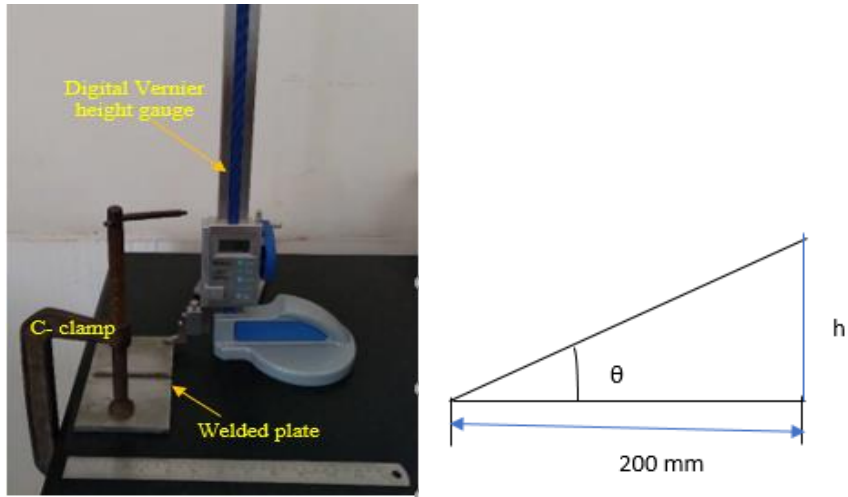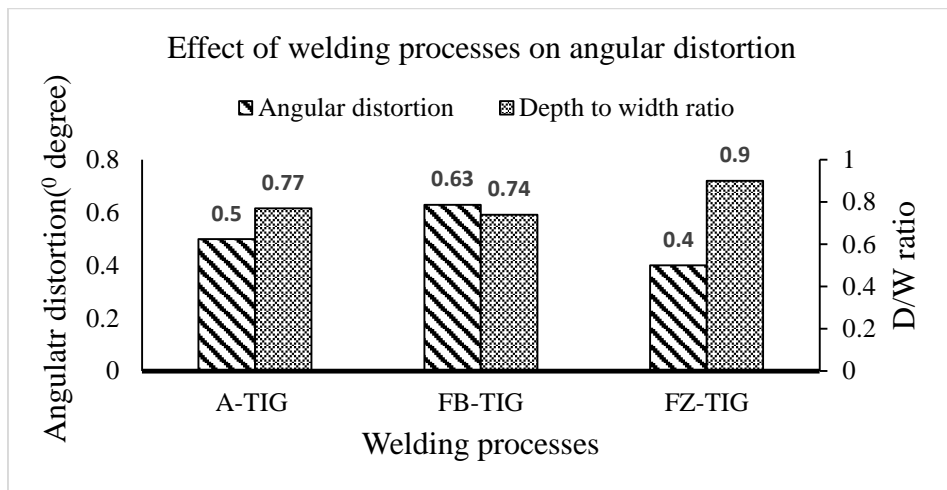
101

Figure 0.9 Measurement of angular distortion

Figure 0.10 Effect of D/W ratio on angular distortion

The activated flux increases the D/W ratio in all welded joints moreover, overheating of base metal is prevented due to a high degree of energy concentration. This may reduce the thermal stress and thereby reduces angular distortion in the weld metal. Moreover, FZ-TIG weld metal indicates the full penetration and D/W ratio near to unity. This shows that volume from top to bottom of the weldment is consistent consequently, angular distortion is negligible.

The Microhardness of the DSS weld depends upon heat input. It was reported that high heat input leads to a slow cooling rate resulting in a larger grain size with higher content of austenite phase which is responsible for the higher hardness of DSS weldments (Paulraj & Garg, 2015). Among all welding (A-TIG, FB-TIG, and FZ-TIG) processes, the highest heat input (reduction in the cooling rate) is observed in FZ-TIG welding and thereby reducing the delta ferrite and courser the grain size. Minimum microhardness

(277HV) is reported with FZ-TIG weld metal as shown in Figure 0.11. Which shows a good correlation between the microhardness and microstructure. A-TIG and FB-TIG weld metal microhardness are higher than base metal this is attributed to the presence of high ferrite than base metal and Widmanstätten secondary austenitic structure. However, FB-TIG welding shows a 13% higher microhardness than the base metal. All 2205 DSS weld metal is failed at the fusion zone. This is due to the formation of coarsening ferrite grains with Widmanstätten austenite during the solidification of A-TIG, FB-TIG, and FZ-TIG weld. In all weld metals, tensile strength is higher than the base metal as shown in Figure 0.11. This is attributed to high heat input, slower cooling rate, and formation of Widmanstätten austenite with high miss-orientation of grain in weld metal zones.
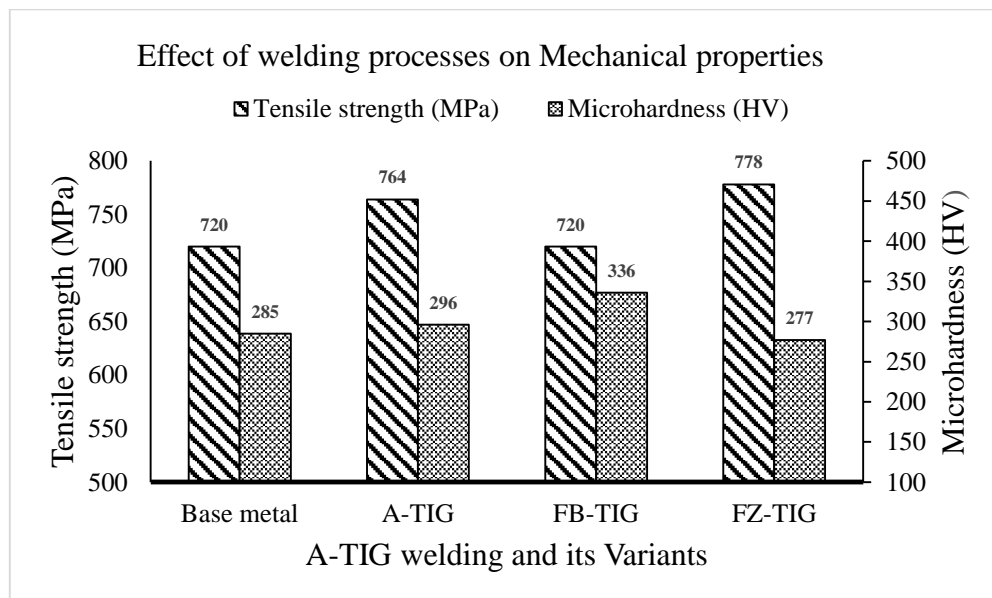

Figure 0.11 Effect of welding process on Mechanical Properties

However, the peak tensile strength of 778 MPA is reported in FZ- TIG butt weld metal. This may be due to the complete and secure penetration with the formation of a large amount of Widmanstätten austenite structure.

6.4.3 Assessment of Electrode tip

The configuration of the welding electrode affects the weld quality observed the higher consumption of electrode in A-TIG welding due to higher amount of arc voltage compared to TIG weld. The weld quality is also affected by the configuration of the welding electrode (Hiraoka, Okada, & Inagaki, 1985; Mills & Keene, 1990). Across the weld pool more even current distribution was observed with frustum and wedge tip

electrodes compared to conical tipped electrodes consequently, the intensity of Marangoni and electromagnetic forces reduces (Poloskov, Erofeev, & Logvin, 2006). The consumption of electrodes is more in A-TIG welding due to the higher amount of arc voltage compared to TIG weld (Tseng & Hsu, 2011).

In the present work, Thoriated Tungsten (EWTh-2) electrode is selected with 2.5 mm diameter having a conical tip angle of 45^0. The electrode tip study has been performed after A-TIG, FB-TIG and FZ-TIG butt welding (100 mm length) using electrode negative TIG power supply at the aforementioned welding parameters. After A-TIG and FZ-TIG welding, almost similar reduction in electrode diameter as shown in Figure 0.12.
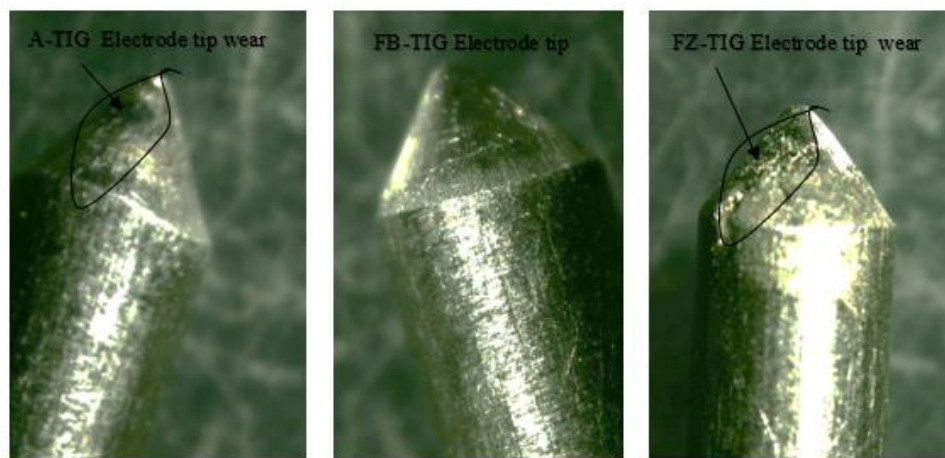

Figure 0.12 Electrode tip appearance after A-TIG, FB-TIG and FZ-TIG welding

This is attributed to strong arc constriction due to peak temperature. Whereas, after FB-TIG welding negligible reduction in electrode diameter is observed. Because FB-TIG welding is performed at a predetermined flux gap and activated flux mostly act as an insulator. Therefore, the electrode tip does not directly come in contact with weld electrodes such as A-TIG and FZ-TIG welding. As a result, it is summarized that a larger electrode diameter (3.2 mm) is more suitable to perform A-TIG and FZ-TIG welding to avoid electrode consumption.

6.4.4 Weld bead Aesthetic appearance

The welded surface is cleaned with acetone after welding to remove the residual flux and to observe the weld bead appearance. The weld bead appearance of A-TIG, FB-TIG and FZ-TIG weld beads are shown in Figure 0.13. In A-TIG welding activated flux hinder the arc movement as fluxes are good insulator and thereby to identify the least

resistive path, the arc is wandering and spatter sideways. Therefore, the A-TIG weld surface becomes more spatter and a thick layer of residual slug (Oxide flux) is observed. Whereas clean weld is observed in FB-TIG weld. Venkatesan et al. (2017) also reported the clean and smooth weld bead with SiO_2 and Cr_2O_3 flux after FB-TIG welding in 304L stainless steel. In FB-TIG welding, a layer of oxide flux on both sides of the flux gap prevents the wondering of the arc column. Therefore, arc energy concentrated close to the gap only consequently, better weld aesthetic appearance is observed. FZ-TIG weld bead appears with a thin layer of the oxide film which is lesser than the A-TIG weld bead. This attribute to strong arc constriction formed by two different flux combinations having unique physical and chemical properties
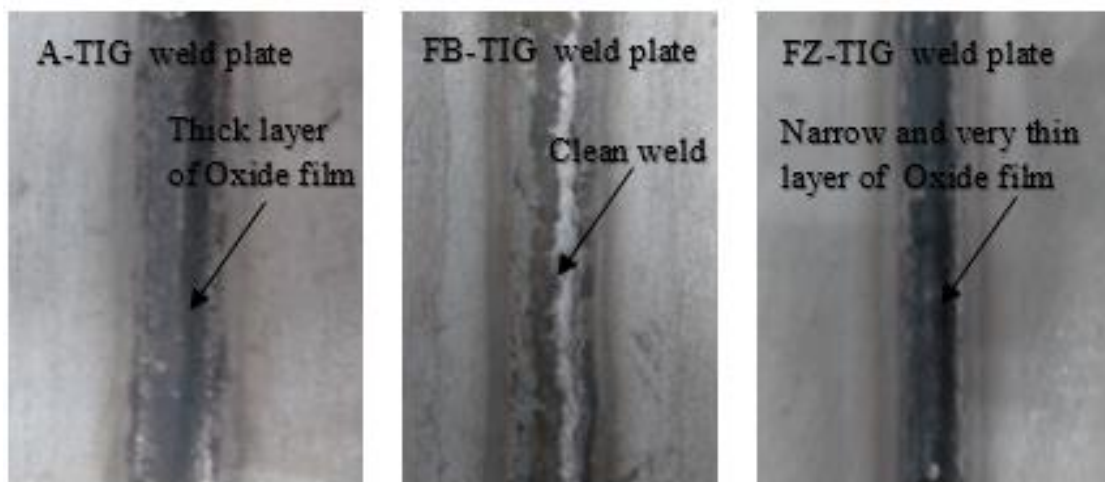

Figure 0.13 Weld bead appearance of A-TIG, FB-TIG and FZ-TIG weld joint

6.5 Summary

In the present investigation comparison of A-TIG weld metal with its variants in 2205 duplex stainless steel are analyzed and summarized as follows:
 The best flux combination for FZ-TIG welding is SiO_2 and Cr_2O_3 fluxes for the inner and outer region of weld bead surface respectively. Maximum penetration is reported 6.9 mm on a 6 mm thick plate which is more than A-TIG and FB-TIG weld metal. However, at 8 mm thick plate reduction in (6.1 mm) penetration is reported. That is attributed to This is due to heat dissipation area increasing with the plate thickness so, plate thickness affects adversely to D/W ratio. Due to substantial increment in D/W ratio in A-TIG and FZ-TIG weld metal, reduces the angular distortion. Among all welding processes, maximum heat input is reported in FZ-TIG welding. Which is

responsible for lesser microhardness due to less delta ferrite. In all weld metal formation of Widmanstätten austenite with high miss-orientation of grain is observed. Which is responsible for higher tensile strength than the base metal. Moreover, compete and secure penetration in A-TIG and FZ-TIG welding increase the weld tensile properties. After A-TIG and FZ-TIG welding, the almost similar reduction is observed in electrode diameter Whereas, after FB-TIG welding negligible reduction is reported. FZ-TIG weld bead appears with a thin layer of oxide file which is battered compared to A-TIG weld bead. This is attributed to two different flux combinations having different physical and chemical properties.